

Inhibition of Hepatitis C Virus NS3 Helicase by Manoalide

Kazi Abdus Salam,[†] Atsushi Furuta,^{‡,§} Naohiro Noda,^{‡,§} Satoshi Tsuneda,[‡] Yuji Sekiguchi,[§] Atsuya Yamashita,[⊥] Kohji Moriishi,[⊥] Masamichi Nakakoshi,^{||} Masayoshi Tsubuki,^{||} Hidenori Tani,[†] Junichi Tanaka,[▽] and Nobuyoshi Akimitsu^{†,*}

[†]Radioisotope Center, The University of Tokyo, 2-11-16 Yayoi, Bunkyo-ku, Tokyo 113-0032, Japan

[‡]Department of Life Science and Medical Bio-Science, Waseda University, 2-2 Wakamatsu-cho, Shinjuku-ku, Tokyo 162-8480, Japan

[§]Biomedical Research Institute, National Institute of Advanced Industrial Science and Technology (AIST), 1-1-1 Higashi, Tsukuba, Ibaraki 305-8566, Japan

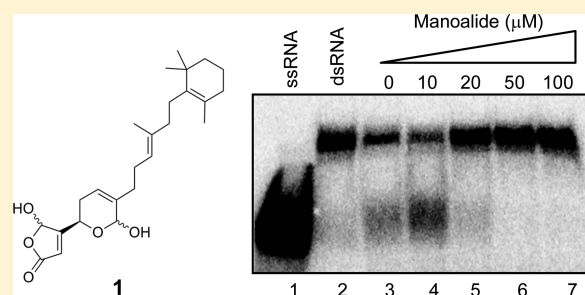
[⊥]Department of Microbiology, Graduate School of Medicine and Engineering, University of Yamanashi, 1110 Shimokato, Chuo-shi, Yamanashi 409-3898, Japan

^{||}Institute of Medical Chemistry, Hoshi University, Ebara 2-4-41, Shinagawa-ku, Tokyo 142-8501, Japan

[▽]Department of Chemistry, Biology and Marine Science, University of the Ryukyus, Nishihara, Okinawa 903-0213, Japan

Supporting Information

ABSTRACT: The hepatitis C virus (HCV) causes one of the most prevalent chronic infectious diseases in the world, hepatitis C, which ultimately develops into liver cancer through cirrhosis. The NS3 protein of HCV possesses nucleoside triphosphatase (NTPase) and RNA helicase activities. As both activities are essential for viral replication, NS3 is proposed as an ideal target for antiviral drug development. In this study, we identified manoalide (**1**) from marine sponge extracts as an RNA helicase inhibitor using a high-throughput screening photoinduced electron transfer (PET) system that we previously developed. Compound **1** inhibits the RNA helicase and ATPase activities of NS3 in a dose-dependent manner, with IC₅₀ values of 15 and 70 μM, respectively. Biochemical kinetic analysis demonstrated that **1** does not affect the apparent K_m value (0.31 mM) of NS3 ATPase activity, suggesting that **1** acts as a noncompetitive inhibitor. The binding of NS3 to single-stranded RNA was inhibited by **1**. Manoalide (**1**) also has the ability to inhibit the ATPase activity of human DHX36/RHAU, a putative RNA helicase. Taken together, we conclude that **1** inhibits the ATPase, RNA binding, and helicase activities of NS3 by targeting the helicase core domain conserved in both HCV NS3 and DHX36/RHAU.



Hepatitis C is an infectious liver disease caused by the hepatitis C virus (HCV) that leads to liver fibrosis, cirrhosis, and finally hepatocellular carcinoma in 2–4% of all of cases.¹ Liver transplantation is the only chance of survival at late stage cirrhosis, resulting in significant increases in transplantations in many countries. More than 170 million people are infected with HCV, corresponding to 3% of the world's population, and 3 to 4 million people are infected each year.^{2–4} Overall, HCV contributes to between 50% and 76% of all liver cancers and two-thirds of liver transplants in developed countries.⁵ Today, HCV is one of the major global health issues.

Current therapy with pegylated interferon- α and ribavirin is the best choice, although it is only effective in approximately 50% of the patients. This combined therapy is expensive, is associated with serious side effects, and requires long-term administration.^{6–8} Unfortunately, no vaccine is available due to the fact that HCV is rapidly mutable, allowing the virus to escape from the neutralizing antibodies, but attempts are

continuing. Therefore, novel antiviral drugs are urgently needed.

HCV is a single-stranded positive sense RNA virus belonging to the family *Flaviviridae*^{9,10} with seven genotypes and more than 50 subtypes. The viral genome comprises about 9.6 kb including a 5'-untranslated region (UTR) with an internal ribosomal entry site, an open reading frame encoding a single polypeptide of 3000 amino acids, and a 3'-UTR.¹¹ The polypeptide, in the sequence of C-E1-E2-p7-NS2-NS3-NS4A-NS4B-NS5A-NS5B, undergoes co- and post-translational cleavage by both viral and cellular proteases to form 10 individual proteins. The structural proteins C to E2 are involved in the formation of the viral capsid and envelope, while nonstructural proteins p7 to NS5B are responsible for viral replication. Among them, NS3 is a multifunctional protein of 631 amino acids and two domains. The N-terminal domain (aa 1–180) has serine protease activity, whereas the C-terminal

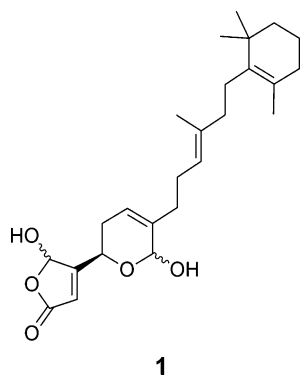
Received: November 8, 2011

Published: March 6, 2012

domain (aa 181–631) exhibits RNA helicase activity.^{12,13} Like other helicases, NS3 helicase possesses NTPase (nucleoside triphosphatase) activity, which is essential for their translocation and unwinding of double-stranded RNA (dsRNA) in a 3' to 5' direction during replication of viral genomic RNA. Therefore, NTPase/helicases, such as the NS3 protease, are promising targets for developing directly acting antiviral chemotherapy.

Telaprevir and boceprevir are two NS3 protease inhibitors that were recently approved by the FDA for use as a triple therapy in combination with pegylated interferon- α and ribavirin for the treatment of chronic genotype 1 HCV infections.^{14,15} This triple therapy improved the SVR (sustained virologic response) up to 70–80% of the current standard of care with minor adverse reactions: mainly rashes, anemia, and nausea. In contrast, no ideal RNA helicase inhibitor has been approved in clinical trials.

Manoalide (**1**) is a marine natural product, first isolated in the early 1980s from the sponge *Luffariella variabilis*.¹⁶ It is a member of a chemical family known as the sesterterpenes. Although this natural product was originally reported as an antibiotic, follow-up work revealed that manoalide possesses promising anti-inflammatory properties.¹⁷ Manoalide (**1**) was reported as the first marine natural product inhibiting the phospholipases A₂ (PLA₂s). PLA₂s play an important role in the inflammation process. To date **1** is the most investigated marine PLA₂ antagonist. It also inhibits calcium channels, 5-lipoxygenase, and phospholipase C.^{18–20} No antiviral activity of **1** has been reported yet. In this study, we identified **1** by screening marine organism extracts and characterized its HCV NS3 helicase inhibitory activity. We found that **1** acts through the inhibition of NS3 ATPase activity and RNA binding.



RESULTS AND DISCUSSION

To obtain potential NS3 helicase inhibitors from extracts of marine organisms, we performed photoinduced electron transfer (PET)-based high-throughput screening.²¹ From 23 extracts of marine organisms, number 2 significantly decreased the activity of NS3 helicase (Table S1, Supporting Information), suggesting the presence of a potential NS3 helicase inhibitor. The presence of **1**¹⁶ was identified in sample 2 by comparing its NMR spectra with those previously reported for **1**.²² We then examined the activity of commercially available **1** against NS3 helicase. We found that the inhibition of NS3 helicase activity by **1** corresponded to that seen with the extract, indicating that **1** provides the main helicase inhibitory activity of sample 2 (data not shown).

To confirm the inhibitory activity of **1** against NS3 helicase, we examined the effect of **1** in an RNA helicase assay using ³²P-labeled dsRNA as a substrate. As shown in Figure 1A, **1** inhibited the dsRNA unwinding, with an approximate IC₅₀ value of 15 μ M.

To determine the effect of **1** on ATPase activity of NS3, we measured the released inorganic phosphate from radioisotope-labeled ATP. The hydrolysis of ATP catalyzed by NS3 was inhibited in a dose-dependent manner by **1** (Figure 1B and C) with an IC₅₀ value 70 μ M. Next, we examined the effects of **1** at varying ATP concentrations with fixed amounts of NS3 (300 nM) and poly(U) RNA (0.1 μ g/ μ L) to determine whether **1** competes with ATP for the same binding site on NS3. The Lineweaver–Burk equation was used to determine K_m value in the presence and absence of **1**. In Figure 2, the intercepts of the x -axis and the y -axis on the Lineweaver–Burk double reciprocal plot indicate $-1/K_m$ and $1/V_{max}$, respectively. The Lineweaver–Burk double reciprocal plot showed that the apparent K_m value was not changed by **1**. In contrast, V_{max} was altered in the presence of **1**. These data indicate that **1** exhibits noncompetitive-type inhibition.

We also determined the effects of **1** on the ATPase activity of human DHX36/RHAU, a putative RNA helicase whose ATPase activity is required for mRNA deadenylation and degradation.²³ Manoalide (**1**) inhibited the ATPase activity of DHX36/RHAU at the same concentration of **1** required to inhibit the ATPase of NS3 (Figure 3A). Both proteins belong to superfamily 2 (SF2), and they share a catalytic core with high structural similarity to a helicase motif (Figure 3B).²⁴ Our results suggested that **1** binds to the conserved helicase motif and interferes with the ATPase of helicases.

As binding of NS3 to single-stranded regions of substrate RNA is required for its unwinding activity, we tested whether **1** inhibits the binding of NS3 to ssRNA. We employed a gel mobility shift assay (GMSA) to determine the binding activity of NS3 to human lethal-7 (let-7) microRNA precursor ssRNA. We found that NS3 binding to ssRNA was inhibited by **1** (Figure 4, lane 4). Because poly(U) RNA enhances the ATPase activity of NS3,²⁵ there is a possibility that the inhibition of NS3 ATPase activity by **1** is caused by inhibition of poly(U) RNA binding. To test this possibility, we performed an ATPase assay in the absence of poly(U) RNA (Figure 5). ATPase activity of NS3 was inhibited by **1** in the absence of poly(U) RNA, ruling out this possibility.

Drugs targeting the unwinding activity could act via one or more of the following mechanisms:²⁶ (a) inhibiting ATPase activity by interfering with ATP binding and therefore limiting the energy available for the unwinding, (b) inhibiting ATP hydrolysis or release of ADP by blocking opening or closing of domains, (c) inhibiting RNA (or DNA) substrate binding, (d) inhibiting unwinding by sterically blocking helicase translocation, or (e) inhibiting coupling of ATP hydrolysis to unwinding. This study shows that **1** inhibits the ATPase and RNA binding capability of NS3, suggesting that **1** may possess two modes of inhibitory action on NS3 activity. Structural analysis of NS3 revealed that the regions contacting the substrate RNA binding domain and the ATP binding domain are located on opposite faces and are not close to each other.²⁷ As **1** is a small molecule, it cannot simultaneously mask the RNA binding domain and ATP binding domain. Therefore, we speculate that **1** binds to a certain core helicase motif and interferes with the ATPase through a structural change of the helicase domain (Figure 6 and Figure S1, Supporting

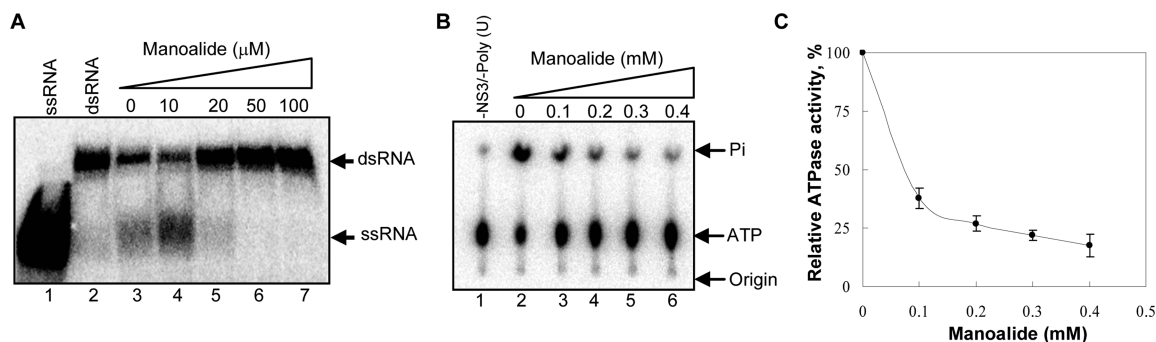


Figure 1. Inhibition of NS3 helicase and ATPase activity by manoolide. (A) The inhibitory effect of manoolide on NS3 helicase activity was determined as described in the Experimental Section. Lane 1 shows the heat-denatured ssRNA (26-mer), and lane 2 shows the partial duplex RNA substrate. Lanes 3–7 show the reactions containing NS3 (300 nM) with increasing concentrations of manoolide (lane 3, 0 μ M; lane 4, 10 μ M; lane 5, 20 μ M; lane 6, 50 μ M; lane 7, 100 μ M). (B) The reaction mixtures were incubated with [γ - 32 P] ATP as described in the Experimental Section. Lane 1 contains a control reaction mixture in the absence of NS3 and poly(U) RNA. Lane 2 shows the reaction mixture containing only NS3 (300 nM) and 5% DMSO. Lanes 3–6 show the NS3 reaction with increasing concentrations of manoolide (lane 3, 0.1 mM; lane 4, 0.2 mM; lane 5, 0.3 mM; lane 6, 0.4 mM). The origin, migration of input ATP, and NS3-hydrolyzed inorganic phosphate (Pi) are indicated on the right side of the figure. (C) The experiment shown in panel B is represented graphically. Hydrolytic activity in the absence of inhibitor was taken as 100%. Experiments were conducted independently three times, and their means \pm standard deviations were included at each point. An IC_{50} of manoolide of 70 μ M was calculated from this figure.

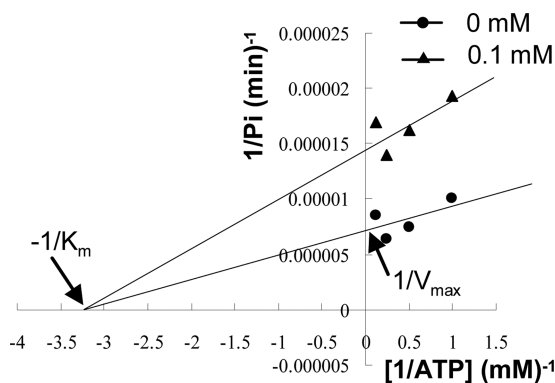


Figure 2. Kinetic profile of manoolide on the inhibition of NS3 ATPase activity. Reactions were performed in 25 mM MOPS–NaOH (pH 7), 1 mM DTT, 5 mM $MgCl_2$, 5 mM $CaCl_2$, 300 nM NS3, and 0.1 μ g/ μ L poly(U) RNA at various [γ - 32 P] ATP concentrations (1, 2, 4, and 8 mM) in the presence of the indicated concentrations of manoolide (0 mM manoolide, filled circles; 0.1 mM manoolide, filled triangles).

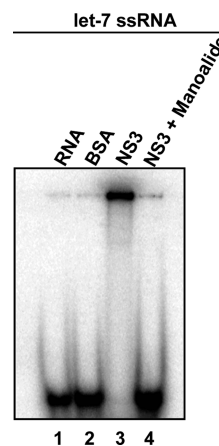


Figure 4. Gel mobility shift assay for the inhibition of NS3 RNA binding. GMSA was performed as described in the Experimental Section. Lanes 1–4 show the GMSA with 1 nM labeled let-7 ssRNA. Heat-denatured RNA alone (lane 1), 300 nM BSA (lane 2), 300 nM NS3 (lane 3), 300 nM NS3 + 0.1 mM manoolide (lane 4).

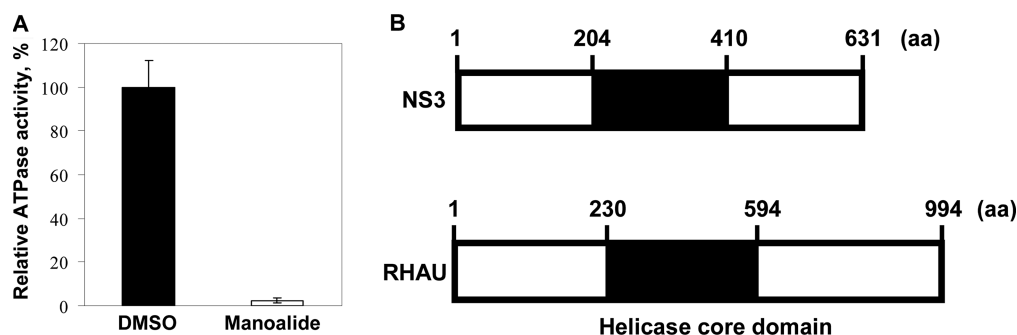


Figure 3. Inhibition of DHX36/RHAU ATPase activity. (A) Reactions were incubated in a buffer solution (50 mM MOPS [pH 7], 2 mM DTT, 3 mM $MgCl_2$) containing 0.5 μ L of RHAU, 0.1 μ g/ μ L poly(U) RNA, 0.1 mM manoolide, and 0.1 mM [γ - 32 P] ATP at 37 $^{\circ}$ C for 30 min. Black and white bars indicate reactions performed in the absence (5% DMSO) or presence of manoolide, respectively. The data are means \pm standard deviations of triplicate assays. (B) Schematic overview of NS3 and RHAU structures. Sequence alignment was carried out on CLUSTALW (<http://www.genome.jp/tools/clustalw/>). Black box indicates the helicase core domain conserved in SF2 helicases. The numbers indicate amino acid residues.

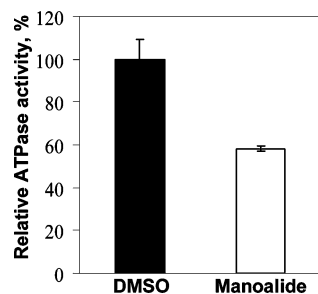


Figure 5. Effects of manoalide on NS3 ATPase activity in the absence of poly(U) RNA. Reaction mixtures contained 25 mM MOPS–NaOH (pH 7), 1 mM DTT, 5 mM MgCl₂, 5 mM CaCl₂, 600 nM NS3, and 0.1 mM manoalide. These were incubated with 1 mM [γ -³²P] ATP in the absence of poly(U) RNA at 37 °C for 60 min. Black and white bars indicate that the reactions were performed in the absence (5% DMSO) or presence of manoalide, respectively. The data are means \pm standard deviations of triplicate assays.

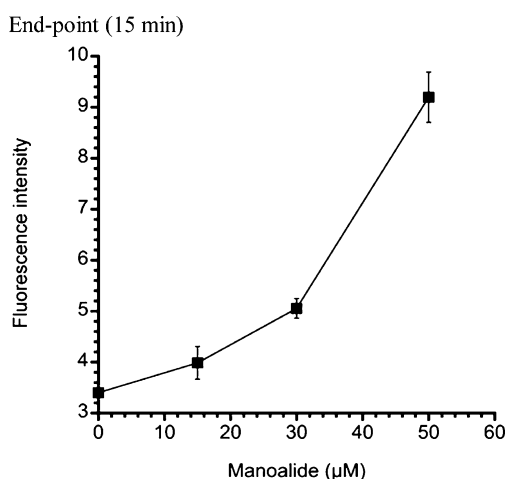


Figure 6. Isothermal denaturation assay (ITD). The ITD assay was performed in 25 mM MOPS–NaOH (pH 6.5), 10 \times concentrated SYPRO orange, and 240 nM NS3 helicase in 20 μ L of reaction mixture with the indicated increasing concentrations of manoalide. The data are means \pm standard deviations of triplicate assays.

Information). To test this idea, we have carried out an isothermal denaturation (ITD) assay, which can assess the stability of proteins at temperatures below the melting temperature and detect the binding of ligands.²⁸ The ITD assay was employed by detecting the increase of fluorescence intensity with the structural change of NS3 as described previously.²⁹ Figure 6 shows that the fluorescence intensity increased in a dose-dependent manner, strongly suggesting that the NS3 structure was changed by the addition of **1**. This result supports the idea that **1** inhibits NS3 activities through the structural changes by direct binding.

Manoalide (**1**) was originally isolated as an inhibitor of beta-bungarotoxin and phospholipase A₂³⁰ but was later found to inhibit calcium channels¹⁸ and 5-lipoxygenase.¹⁹ The hemiacetal in the dihydropyran ring of **1** has been shown to be required for the inhibition of phospholipase A₂.³¹ So far, we do not know if the hemiacetal is also essential for the inhibition of NS3. We speculate that acetal formation between a hemiacetal residue of **1** and a serine and/or threonine residue of the helicase core domain, which contains many evolutionarily conserved serine and threonine residues, may occur. Future structural and functional analyses will reveal the essential

structure of **1** required to inhibit NS3, allowing the development of specific inhibitors to NS3 but not phospholipase A₂.

EXPERIMENTAL SECTION

Preparation of Extracts from Marine Organisms. Specimens of marine sponges were collected in Okinawa, Japan (Table S1, Supporting Information). The specimens were extracted three times with either EtOH or acetone, and the EtOAc-soluble portions were obtained after concentration and partition.

Chemicals. Manoalide was purchased from Santa Cruz Biotechnology. γ -³²P-ATP and γ -³³P-ATP were purchased from Muromachi Yakuhin and PerkinElmer, respectively. Let-7 ssRNA was synthesized by Gene Design Inc. Poly (U) RNA was obtained from Sigma-Aldrich.

High-Throughput Screening of NS3 Helicase Inhibitors. The fluorescence helicase activity assay based on photoinduced electron transfer was performed as described in our previous study²¹ with modifications of the substrate and the composition of the reaction mixture.

The substrate was prepared as dsRNA by annealing, at a 1:2 molar ratio, a 5' BODIPY FL-labeled 37-mer (5'-CUAAUACCUCCACC-CUCAUAACCUUUUUUUUUUUUUU-3') to a 23-mer (GGUUAU-GAGGGUGGAGGUAUAG). When unwound by HCV NS3 helicase, the unlabeled ssRNA is captured by a DNA capture strand (5'-CTATTACCTCCACCCTCATAACC-3'). A fluorescent-dye-labeled oligonucleotide was purchased from J-Bio 21 Corporation. BODIPY FL was attached to the 5'-end via an aminohexylphosphate linker with a six-carbon spacer. Unlabeled oligonucleotides were purchased from Japan Bio Services Co., Ltd.

The continuous fluorescence assay was performed in 25 mM MOPS–NaOH (pH 6.5), 3 mM MgCl₂, 2 mM DTT, 4 U RNasin (Promega), 50 nM dsRNA substrate, 100 nM DNA capture strand, and 5 mM ATP in 20 μ L of reaction mixture. The diluted extracts in DMSO were added (2 μ L) to the reaction mixtures to a final concentration of 15–35 μ g/mL. The reaction was started by adding 240 nM HCV NS3 helicase, which was expressed and purified as described previously,²¹ and performed at 37 °C for 30 min using a LightCycler 1.5 (Roche). The fluorescence intensity was recorded every 5 s from 0 to 5 min and then every 30 s from 5 to 30 min. The activity of NS3 helicase was calculated as the initial reaction velocity. Inhibition was calculated relative to the control value examined without inhibitors but with DMSO.

ATPase Assay. NS3 ATPase activity was directly determined by monitoring [γ -³²P] ATP hydrolysis by thin-layer chromatography. The assays were performed as previously described³² with slight modifications. Unless otherwise specified, the standard assay mixture contained 25 mM MOPS–NaOH (pH 7.0), 1 mM DTT, 5 mM MgCl₂, 5 mM CaCl₂, 1 mM [γ -³²P] ATP (PerkinElmer), 300 nM NS3, and 0.1 μ g/ μ L poly(U) with the indicated increasing concentrations of manoalide in a reaction volume of 10 μ L. Reactions were conducted at 37 °C for 10 min and stopped by the addition of stop solution (10 mM EDTA). A 2 μ L amount of each reaction mixture was spotted onto polyethyleneimine cellulose sheets (Merck) and developed in 0.75 M LiCl/1 M formic acid solution for 20 min. The cellulose sheets were dried, and released [³²P] phosphoric acid was visualized with an FLA-9000 image reader and quantified by Multi Gauge V3.11 software (Fujifilm).

RNA Binding Assay. RNA binding was determined by a gel mobility shift assay.³³ First, let-7 ssRNA (5'-UGAGGUAGUAGGUU-GUAUAGU-3') was labeled at the 5'-end with [γ -³²P] ATP (Muromachi) using T4 polynucleotide kinase (Toyobo) at 37 °C for 60 min and purified by the phenol-chloroform extraction method. Each 20 μ L of reaction mixture contained 30 mM Tris-HCl (pH 7.5), 100 mM NaCl, 2 mM MgCl₂, 1 mM DTT, 20 units of RNasin Plus (Promega) that was incubated with 300 nM NS3, 1 nM let-7 labeled ssRNA, and 0.1 mM manoalide at room temperature for 15 min. An equal volume of dye solution [0.025% bromophenol blue, 10% glycerol in 0.5 \times Tris/borate/EDTA (TBE)] was added to each reaction mixture and loaded onto a 6% native-PAGE gel

(acrylamide:bis = 19:1). The labeled RNA bands were visualized with an FLA-9000 image reader (Fujifilm).

RNA Helicase Assay. The NS3 RNA helicase assay was performed as described previously³² with some modifications. Briefly, the substrate for annealing two complementary RNA oligonucleotides, 5'-AGAGAGAGAGGUUGAGAGAGAGAGUUUGAGAGAGAGAGAG-3' (40-mer, template strand) and 5'-CAAACUCUCUCUCUCUCAACAAAAA-3' (26-mer, release strand), was purchased from Shanghai GenePharma Co., Ltd. The release strand was labeled at the 5'-end with [γ -³²P] ATP (Muromachi) using the T4 polynucleotide kinase (Toyobo) at 37 °C for 60 min and purified by phenol-chloroform extraction. The template and the labeled release strands were annealed at a molar ratio of 3:1 (template/release), denatured at 80 °C for 5 min, and slowly renatured at 23 °C for 30 min in an annealing buffer [20 mM Tris-HCl (pH 8), 0.5 M NaCl, 1 mM EDTA]. The partial duplex RNA substrate was purified on a G-50 microcolumn (GE Healthcare) and stored at -20 °C in H₂O containing 0.25 U of RNasin Plus (Promega) per μ L.

The inhibition assay of NS3 RNA helicase activity by manoalide was conducted in 20 μ L of helicase reaction mixture [25 mM MOPS-NaOH (pH 7), 2.5 mM DTT, 2.5 U of RNasin Plus (Promega), 100 μ g of BSA per mL, 3 mM MgCl₂] containing 300 nM NS3 protein and 0.4 nM ³²P-labeled partial duplex RNA substrate with increasing concentrations of manoalide (as indicated) and preincubated at 23 °C for 15 min. After adding 5 mM ATP, the reaction was carried out at 37 °C for 30 min and stopped by adding 5 μ L of helicase termination buffer (0.1 M Tris [pH 7.5], 20 mM EDTA, 0.5% SDS, 0.1% Nonidet P-40, 0.1% bromophenol blue, 0.1% xylene cyanol, 25% glycerol). The inhibition of NS3 helicase activity was analyzed on a 10% native TBE polyacrylamide gel, and the labeled RNAs were visualized with an FLA-9000 image reader (Fujifilm).

Isothermal Denaturation Assay. The effect of manoalide on the structure change of NS3 helicase was measured using the isothermal denaturation assay.²⁹ Briefly, the ITD assay was performed in 25 mM MOPS-NaOH (pH 6.5), 10 \times concentrated SYPRO orange (Molecular Probes, Eugene, OR, USA), and 240 nM NS3 helicase in 20 μ L of reaction mixture with the indicated increasing concentrations of manoalide (Santa Cruz Biotechnology). While SYPRO orange has a low quantum yield in an aqueous environment, the fluorescence intensity increases when the dye binds to the hydrophobic regions exposed upon unfolding of the enzyme. The reaction was carried out in three replicates for each concentration of manoalide at 37 °C for 15 min using a LightCycler 1.5 (Roche) with the fluorescence intensity measured.

■ ASSOCIATED CONTENT

📄 Supporting Information

Summary of NS3 helicase inhibitory activity in extracts of marine sponges and Figure S1. This material is available free of charge via the Internet at <http://pubs.acs.org>.

■ AUTHOR INFORMATION

Corresponding Author

*Phone: +81-3-5841-3057. Fax: +81-3-5841-3049. E-mail: akimitsu@ric.u-tokyo.ac.jp.

Notes

The authors declare no competing financial interest.

■ ACKNOWLEDGMENTS

The authors express gratitude and special thanks to S. Nishikawa (AIST) for his kind gift of the expression plasmid pT7/His-NS3 containing an N-terminal His-tagged full-length HCV NS3.

■ REFERENCES

- (1) Gravit, L. *Nature* **2011**, *474*, S2–S4.
- (2) Butt, A. A. *Expert Rev. Anti-Infect. Ther.* **2005**, *3*, 241–249.

- (3) Soriano, V.; Peters, M. G.; Zeuzem, S. *Clin. Infect. Dis.* **2009**, *48*, 313–320.
- (4) Koziol, M. J.; Peters, M. G. *New Engl. J. Med.* **2007**, *356*, 1445–1454.
- (5) Kai, L. *Virol. Sin.* **2010**, *25*, 246–266.
- (6) McHutchison, J. G.; Gordon, S. C.; Schiff, E. R.; Shiffman, M. L.; Lee, W. M.; Rustgi, V. K.; Goodman, Z. D.; Ling, M. H.; Cort, S.; Albrecht, J. K. *New Engl. J. Med.* **1998**, *339*, 1485–1492.
- (7) Cummings, K. J.; Lee, S. M.; West, E. S.; Cid-Ruzafa, J.; Fein, S. G.; Aoki, Y.; Sulkowski, M. S.; Goodman, S. N. *J. Am. Med. Assoc.* **2001**, *285*, 193–199.
- (8) Tam, R. C.; Lau, J. Y.; Hong, Z. *Antiviral Chem. Chemother.* **2001**, *12*, 261–272.
- (9) Choo, Q. L.; Kuo, G.; Weiner, A. J.; Overby, L. R.; Bradley, D. W.; Houghton, M. *Science* **1989**, *244*, 359–362.
- (10) Takamizawa, A.; Mori, C.; Fuke, I.; Manabe, S.; Murakami, S.; Fujita, J.; Onishi, E.; Anodoh, T.; Yoshida, I.; Oakayama, H. *J. Virol.* **1991**, *65*, 1105–1113.
- (11) Moradpour, D.; Penin, F.; Rice, C. M. *Nat. Rev. Microbiol.* **2007**, *5*, 453–463.
- (12) De Francesco, R.; Steinkühler, C. *Curr. Top. Microbiol. Immunol.* **2000**, *242*, 149–169.
- (13) Raney, K. D.; Sharma, S. D.; Moustafa, I. M.; Cameron, C. E. *J. Biol. Chem.* **2010**, *285*, 22725–22731.
- (14) Burney, T.; Dusheiko, G. *Expert Rev. Anti-Infect. Ther.* **2011**, *9*, 151–160.
- (15) Bacon, B. R.; Gordon, S. C.; Lawitz, E.; Marcellin, P.; Vierling, J. M.; Zeuzem, S.; Poordad, F.; Goodman, Z. D.; Sings, H. L.; Boparai, N.; Burroughs, M.; Brass, C. A.; Albrecht, J. K.; Esteban, R. *New Engl. J. Med.* **2011**, *364*, 1207–1217.
- (16) De Silva, E. D.; Scheuer, P. J. *Tetrahedron Lett.* **1980**, *21*, 1611–1614.
- (17) Newman, D. J.; Cragg, G. M. *J. Nat. Prod.* **2004**, *67*, 1216–1238.
- (18) Wheeler, L. A.; Sachs, G.; De Vries, G.; Goodrum, D.; Woldemussie, E.; Muallem, S. *J. Biol. Chem.* **1987**, *262*, 6531–6538.
- (19) De Vries, G. W.; Amdahl, L.; Mobasser, A.; Wenzel, M.; Wheeler, L. A. *Biochem. Pharmacol.* **1988**, *37*, 2899–2905.
- (20) Bennett, C. F.; Mong, S.; Wu, H. L.; Clark, M. A.; Wheeler, L.; Crooke, S. T. *Mol. Pharmacol.* **1987**, *32*, 587–593.
- (21) Tani, H.; Akimitsu, N.; Fujita, O.; Matsuda, Y.; Miyata, R.; Tsuneda, S.; Igarashi, M.; Sekiguchi, Y.; Noda, N. *Biochem. Biophys. Res. Commun.* **2009**, *379*, 1054–1059.
- (22) Uddin, M. H.; Otsuka, M.; Muroi, T.; Ono, A.; Hanif, N.; Matsuda, S.; Higa, T.; Tanaka, J. *Chem. Pharm. Bull.* **2009**, *57*, 885–887.
- (23) Tran, H.; Schilling, M.; Wirbelauer, C.; Hess, D.; Nagamine, Y. *Mol. Cell* **2004**, *13*, 101–111.
- (24) Fairman-Williams, M. E.; Guenther, U. P.; Jankowsky, E. *Curr. Opin. Struct. Biol.* **2010**, *20*, 313–324.
- (25) Suzich, J. A.; Tamura, J. K.; Palmer-Hill, F.; Warren, P.; Grakoui, A.; Rice, C. M.; Feinstone, S. M.; Collett, M. S. *J. Virol.* **1993**, *67*, 6152–6158.
- (26) Borowski, P.; Deinert, J.; Schalinski, S.; Bretner, M.; Ginals, K.; Kulikowski, T.; Shugar, D. *Eur. J. Biochem.* **2003**, *270*, 1645–1653.
- (27) Gu, M.; Rice, C. M. *Proc. Nat. Acad. Sci. U. S. A.* **2010**, *107*, 521–528.
- (28) Senisterra, G. A.; Hong, B. S.; Park, H. W.; Vedadi, M. *J. Biomol. Screen.* **2008**, *13*, 337–342.
- (29) Sarver, R. W.; Rogers, J. M.; Stockman, B. J.; Epps, D. E.; DeZwaan, J.; Harris, M. S.; Baldwin, E. T. *Anal. Biochem.* **2002**, *309*, 186–195.
- (30) De Freitas, J. C.; Blankemeier, L. A.; Jacobs, R. S. *Experientia* **1984**, *40*, 864–865.
- (31) Glaser, K. B.; de Carvalho, M. S.; Jacobs, R. S.; Kernan, M. R.; Faulkner, D. J. *Mol. Pharmacol.* **1989**, *36*, 782–788.
- (32) Gallinari, P.; Brennan, D.; Nardi, C.; Brunetti, M.; Tomei, L.; Steinkühler, C.; De Francesco, R. *J. Virol.* **1998**, *72*, 6758–6769.
- (33) Huang, Y.; Liu, Z. R. *J. Biol. Chem.* **2002**, *277*, 12810–12815.